



Arellano, P. and Tansey, K. and Balzter, H. and Boyd, Doreen S. (2015) Detecting the effects of hydrocarbon pollution in the Amazon forest using hyperspectral satellite images. *Environmental Pollution*, 205 . pp. 225-239. ISSN 0269-7491

Access from the University of Nottingham repository:

http://eprints.nottingham.ac.uk/29207/1/JofEP_accepted.pdf

Copyright and reuse:

The Nottingham ePrints service makes this work by researchers of the University of Nottingham available open access under the following conditions.

- Copyright and all moral rights to the version of the paper presented here belong to the individual author(s) and/or other copyright owners.
- To the extent reasonable and practicable the material made available in Nottingham ePrints has been checked for eligibility before being made available.
- Copies of full items can be used for personal research or study, educational, or not-for-profit purposes without prior permission or charge provided that the authors, title and full bibliographic details are credited, a hyperlink and/or URL is given for the original metadata page and the content is not changed in any way.
- Quotations or similar reproductions must be sufficiently acknowledged.

Please see our full end user licence at:

http://eprints.nottingham.ac.uk/end_user_agreement.pdf

A note on versions:

The version presented here may differ from the published version or from the version of record. If you wish to cite this item you are advised to consult the publisher's version. Please see the repository url above for details on accessing the published version and note that access may require a subscription.

For more information, please contact eprints@nottingham.ac.uk

Paul Arellano, Kevin Tansey, Heiko Balzter and Doreen S. Boyd (accepted) Detecting the effects of hydrocarbon pollution in the Amazon forest using hyperspectral satellite images. *Environmental Pollution*.

This is the final accepted version of the above article and has been deposited according to guidelines: <http://www.sherpa.ac.uk/romeo/issn/0269-7491/>. The final published version (Arellano, P., Tansey, K., Balzter, H. and Boyd, D.S. (2015) Detecting the effects of hydrocarbon pollution in the Amazon forest using hyperspectral satellite images. *Environmental Pollution*, 205, 225-239) can be found at doi:10.1016/j.envpol.2015.05.041.

1 **Detecting the effects of hydrocarbon pollution in the Amazon forest**
2 **using hyperspectral satellite images**

3 Paul Arellano^{a,b,1}, Kevin Tansey^a, Heiko Balzter^{a,c} and Doreen S. Boyd^d

4 ^a University of Leicester, Department of Geography, Centre of Landscape and Climate
5 Research, University Road, Leicester, LE1 7RH, UK

6
7 ^b YachayTech University, School of Geological Sciences & Engineering, Urcuqui,
8 Ecuador

9 ^c National Centre for Earth Observation, University of Leicester, University Road,
10 Leicester, LE1 7RH, UK

11 ^c University of Nottingham, School of Geography, Nottingham, UK

12 **Corresponding author:** Paul Arellano, University Road, Bennett Building, LE1 7RH,
13 Leicester, UK, (pa134@le.ac.uk or parellano@yachaytech.edu.ec)

14 **Keywords:** Petroleum pollution, hyperspectral remote sensing, Amazon forest,
15 vegetation indices, Yasuni National Park

16 **ABSTRACT**

17 The global demand for fossil energy is triggering oil exploration and production
18 projects in remote areas of the world. During the last few decades, hydrocarbon
19 production has caused pollution in the Amazon forest inflicting considerable
20 environmental impact. Until now it is not clear how hydrocarbon pollution affects the
21 health of the tropical forest flora. During a field campaign in polluted and pristine
22 forest, more than 1100 leaf samples were collected and analysed for biophysical and
23 biochemical parameters. The results revealed that tropical forests exposed to
24 hydrocarbon pollution show reduced levels of chlorophyll content, higher levels of
25 foliar water content and leaf structural changes. In order to map this impact over wider
26 geographical areas, vegetation indices were applied to hyperspectral Hyperion satellite
27 imagery. Three vegetation indices (SR, NDVI and NDVI₇₀₅) were found to be the most
28 appropriate indices to detect the effects of petroleum pollution in the Amazon forest.

¹ Present address: YachayTech University, San Miguel de Urcuqui, Ibarra, Ecuador, Tlf: 593-983-033-541, pa134@le.ac.uk, parellano@yachaytech.edu.ec

29 Capsule:

30 Biophysical and biochemical alterations of vegetation of the Amazon forest caused by
31 petroleum pollution can be detected from space using hyperspectral remote sensing.

32 **1. Introduction**

33 Global demand for energy is triggering oil and gas exploration and production across the
34 Amazon basin, with even very remote areas leased out or under negotiation for access
35 (Finer et al. 2008). In western Amazonia, there has been an unprecedented rise in this
36 activity, causing environmental pollution in vast regions of forest via oil spills from
37 pipelines networks and leakages from unlined open pits (Hurtig&San-Sebastián 2005,
38 Bernal 2011). In some cases this has led to legal actions by local residents against
39 international oil companies (Bernal 2011, Rochlin 2011). Currently in Ecuador the
40 petroleum industry and its environmental/social interactions are at the centre of
41 controversy since very sensitive regions and protected areas of this Amazon forest are
42 under exploration and production (Marx 2010, Martin 2011, Vallejo et al. 2015).

43 Despite high international public interest in protecting Amazon rainforests, little
44 scientific attention has focussed on the effects of oil pollution on the forest; much focus
45 is on threats from deforestation, selective logging, hunting, fire and global and regional
46 climate variations (Malhi et al. 2008, Davidson et al. 2012, Asner et al. 2004). The high
47 diversity and intrinsic complex biological interactions of tropical forests and their vast
48 expanse challenge our understanding of the impact of oil on them. Data collected *in situ*
49 in these forests are rare, most likely due to access issues. An alternative approach to
50 measuring and monitoring oil contamination in tropical forests at suitable spatial and
51 temporal scales is desirable. It is suggested here that satellite imaging spectrometry,
52 which affords the collection of hyperspectral data of the environment, could be a way
53 forward. In order to detect vegetated landscape contamination using imaging

54 spectrometry, environmental change as a result of contamination need to have a
55 measurable impact upon the biochemical, and related biophysical properties (e.g.,
56 pigment concentration, leaf structural and leaf area), of the vegetation growing in that
57 environment. Such properties measured using hyperspectral remotely sensed data may
58 then be used as a proxy to contamination (Mutanga;Skidmore & Prins 2004).

59 Experimental data generated under controlled conditions have demonstrated that
60 plants exposed to pollutants exhibit stress symptoms (Horvitz 1982, Smith;Colls &
61 Steven 2005, Horvitz 1985) which manifest themselves primarily in lower levels of
62 chlorophyll content. Stress levels do, however, depend on plant tolerance to both
63 concentration and exposure period (Smith;Steven & Colls 2005, Noomen et al. 2006).
64 There is now an increasing availability of hyperspectral remotely sensed data from
65 space (Hyperion on board of Earth Observation EO-1; Compact High Resolution
66 Imaging Spectrometer-CHRIS on board of PROBA-1) and more are imminent at the
67 time of writing (e.g. Sentinel-2; Environmental Mapping and Analysis Program
68 (EnMAP)). The development of techniques to utilise these data sets for the detection of
69 specific pollutants in a tropical forest environment is necessary and forms the focus of
70 this study. Approaches to using these data include the use of both broad- and narrow-
71 band vegetation indices (e.g., (Blackburn 2007)) and red edge position location (e.g.,
72 (Dawson&Curran 1998)). Their success may vary between species and pollutant
73 (Steven et al. 1990, Sims&Gamon 2002), however, previously these techniques have
74 been used to detect vegetation contamination by heavy metals (Kooistra et al. 2003,
75 Rosso et al. 2005), radioactive materials (Davids&Tyler 2003, Boyd et al. 2006), as
76 well as hydrocarbons (Smith;Steven & Colls 2005, Jago;Cutler & Curran 1999,
77 Noomen et al. 2008, Noomen&Skidmore 2009, Zhu et al. 2013) and herbicides
78 (Dash&Curran 2006).

79 ***1.1 Vegetation stress caused by crude oil***

80 Vegetation responds to stress conditions with long-term metabolic and morphological
81 changes: these include changes in the rate of photosynthesis, changes in the absolute and
82 relative concentration of the photosynthetic pigment (chlorophyll a and b, carotenoids)
83 and changes in leaf size, thickness and structure (Davids&Tyler 2003). Different plant
84 species respond differently to a particular stressor. Furthermore, the nature, intensity
85 and length to exposure are factors that define the stress level on the vegetation. Baker
86 (1970) summarised several pieces of research related to the effects of crude-oil on
87 plants and showed that the toxicity of petroleum oil depends on the concentration of
88 unsaturated, aromatics and acids compounds: the higher their concentration, the more
89 toxic the oil is for plants. Molecules of crude-oil can penetrate the plant through its leaf
90 tissue, stomata, and roots. The rate of penetration depends on the oil type, the contact
91 part (leaves, roots), time of exposure, thickness of the cuticle and the density of the
92 stomata. After penetrating into the plant, the oil may travel into the intercellular space
93 and possibly also into the vascular system. Cell membranes are damaged by the
94 penetration of hydrocarbon molecules leading to the leakage of cell contents, and the
95 possible entry of oil into the cells.

96 Plant transpiration, respiration and photosynthetic rates are affected by
97 hydrocarbon pollution (Baker 1970). The effects of hydrocarbons in plants reduce plant
98 transpiration rates. On the other hand, plant respiration may either decrease or increase
99 depending on the plant species or the oil type. Hydrocarbons reduce the rate of
100 photosynthesis, and the amount of reduction varies with the type and amount of oil and
101 with the species of plant. Cell injury may be the principal cause of photosynthesis
102 inhibition because hydrocarbons tend to accumulate in the chloroplasts, which explains
103 the reduced levels of chlorophyll content in vegetation affected by hydrocarbons.

104 *1.2 Vegetation stress and chlorophyll*

105 The interaction between hydrocarbons and the soils reduces the amount of oxygen and
106 increases the CO₂ concentration, soils turn acidic and minerals are mobilised. These
107 changes affect the vegetation health (Noomen et al. 2006, Shumacher 1996, Yang 1999,
108 van der Meer;Yang & Kroonenberg 2006). Controlled experiments in the laboratory,
109 most of them being applied to crops, have demonstrated that plants exposed to
110 hydrocarbons experience reduced levels of chlorophyll which is a key parameter to
111 detect plant stress caused by hydrocarbons (Smith;Colls & Steven 2005, Smith;Steven
112 & Colls 2005, Noomen&Skidmore 2009, Yang 1999, Smith;Steven & Colls 2004,
113 Noomen 2007). It is not clear how hydrocarbons influence changes in biophysical and
114 biochemical parameters of vegetation growing in natural environments. At present,
115 there are no published studies that investigate the effects of hydrocarbons in vegetation
116 of tropical forest in the Amazon region.

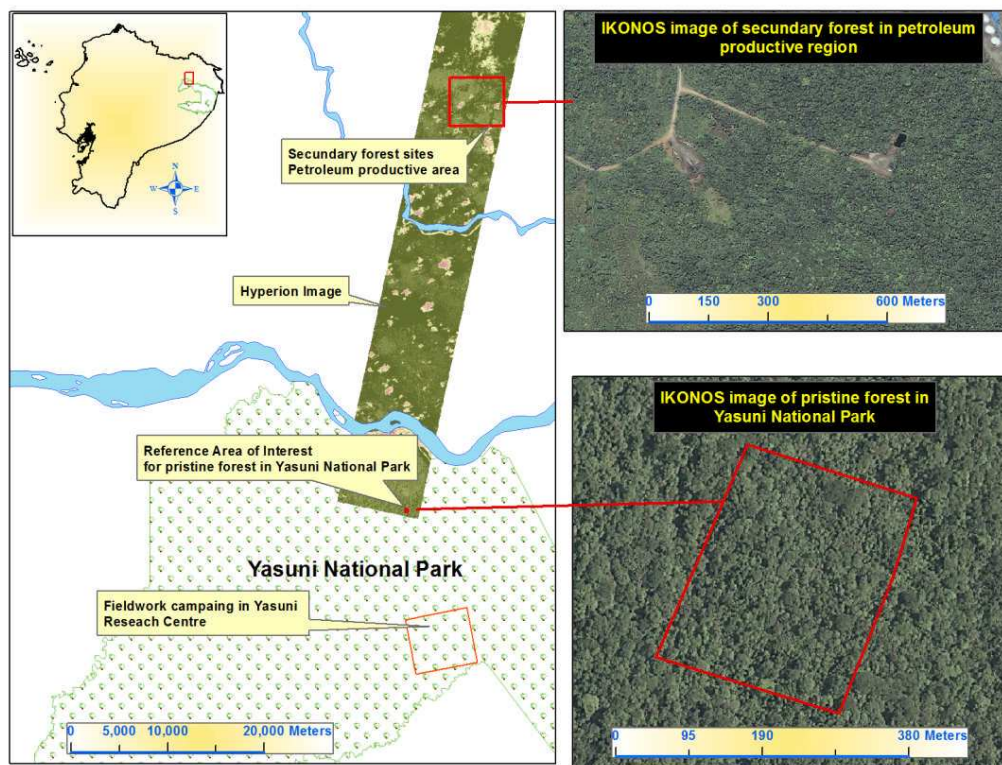
117 This paper demonstrates the suitability of satellite imaging spectrometry for the
118 detection of contamination by oil of the forest in the Ecuadorian Amazon. EO-1 (Earth-
119 Observation 1) Hyperion imagery is analysed with supporting field data on soils and
120 foliar properties with an overriding objective of producing a map of the spatial pattern
121 of forest contamination by oil.

122 **2. Materials and methods**

123 *2.1. Study area and sites*

124 Three study sites within Ecuadorian Amazon rainforest were investigated
125 (Figure **1Error! Reference source not found.**). Two were located in the lowland
126 evergreen secondary forest of Sucumbios province, in the Tarapoa region (0°11' S,
127 76°20' W). Due to their close proximity, both sites share soil types, weather and

128 anthropogenic influences. Site 1 (polluted) is located by an abandoned petroleum
129 platform where open pits have been discharging crude oil to the environment, or
130 leaching out as the pits degrade or overflow, for the past 15 years. Site 2 (non-polluted)
131 is some distance from Site 1 and so not directly influenced by the oil pollution evident
132 at Site 1. Site 3 (Pristine forest-Yasuni) is situated in the highly diverse lowland
133 evergreen primary forest of the Orellana province, in the northern section of Ecuador's
134 Yasuni National Park (0°41' S, 76°24' W). The forest has a species richness among the
135 highest globally (Tedersoo et al. 2010) and are situated well away from any sources of
136 crude oil (and other anthropogenic influences).



137
138

Figure 1. Location of the sampled sites in the Amazon region of Ecuador.

139 2.2. Site sampling and measurements

140 Fieldwork was undertaken from April to July 2012. From each of the three sites
141 two sets of data were collected to measure any oil presence and potential contamination.
142 One set focused on the measurement of levels of oil in the soil. Eight soil samples,

143 randomly situated, were collected at each of the three sites and several parameters
144 related to physical properties, nutrients, metals and hydrocarbons traces were analysed
145 in accredited laboratories following international standard methods (see Annex 1 for
146 details of soil sampling and results). The other set of data focused on measuring the
147 foliar biochemistry of leaves from the trees located at each site. At Site 1 all trees
148 located around the source of oil were sampled (388 samples); at Site 2 selectively
149 sampled areas located between 400 and 1250 meters from Site 1 were the focus of
150 measurement (124 samples); and in Site 3 accessible trees were sampled from 12
151 parcels of 20x20 m which covered an area of 4800 m² (545 samples). In total, therefore
152 1,057 trees were sampled (see Annex 2 and Annex 3 for a detailed description of the
153 plant family and specie sampled). From each tree well-developed branches, acquired
154 from different levels of the vertical forest profile using a telescopic pruner, tree-
155 climbing techniques and canopy towers, were sealed in large polyethylene bags and
156 stored in ice coolers.

157 Fully expanded mature leaves, with no herbivorous/pathogenic damage, were selected
158 from each of the collected branches and analysed. Each leaf was clipped at the midpoint
159 using cork borers to obtain a disk of known surface (S); this is the optimal position from
160 which to take chlorophyll readings (Hoel 1998). Three SPAD-502 chlorophyll meter
161 readings were taken from each disk, at different positions, to compute a mean index
162 value. The fresh weight (Fw) and dry weight (Dw) of each leaf disk were then
163 calculated to measure (i) leaf water content (Cw) in $g\ cm^{-2} = (Fw - Dw) / S$ (Gerber et al.
164 2011, Hunt Jr&Rock 1989, Datt 1999, Féret et al. 2011). Other leaf properties computed
165 were (ii) dry matter content (Cm) in $g\ cm^{-2} = Dw / S$ (Gerber et al. 2011, Datt 1999, Féret
166 et al. 2011); (iii) Specific leaf area (SLA) in $cm^2\ g^{-1} = 1 / Cm$ (Marenco;Antezana-Vera &
167 Nascimento 2009, White&Montes-R 2005, Vile et al. 2005, Sánchez-Azofeifa et al.

168 2009) ; (iv) Leaf water content (*LWC*) in % = (Fw-Dw)/Fw (Marenco;Antezana-Vera
169 & Nascimento 2009); (v) Leaf dry matter content (*LDMC*) in % = Dw/Fw (Vile et al.
170 2005); and (vi) Leaf thickness or leaf succulence (*Lt*) in g cm⁻² = 1/SLA*LDMC (Vile
171 et al. 2005).

172 **2.3. Hyperion image pre-processing**

173 USGS EO-1 Hyperion image acquisition was requested for the time of the
174 fieldwork campaign but cloudy conditions prevented new acquisitions, and therefore the
175 only available Hyperion image was that acquired on 15th February 2005 and this was the
176 focus of investigation. Hyperion data have a spatial resolution of 30m² with each pixel
177 covering the spectral range, 400-2500 nm. A single image is 7.65 km wide (cross-track)
178 by 185 km long (along-track), and this meant that the single image available covered
179 Sites 1 and 2 but not Site 3. Since Site 3 was located in a pristine, uncontaminated
180 rainforest, a reference area of interest located 13km north from the sampled area was
181 chosen inside the Yasuni National Park, with the assumption that the same forest
182 conditions are present for comparative purposes (see Figure 1). Since the Hyperion
183 sensor operates from a satellite platform, pre-processing was undertaken to manage
184 sensor and processing noise and retrieve reflectance for each waveband for use in
185 subsequent analyses: pre-processing included waveband selection, atmospheric and
186 smile effect corrections and noise reduction.

187 Wavelength selection: Hyperion data have 242 spectral bands; 51 bands are not
188 radiometrically calibrated and consequently were not used (1 to 8 (visible); 58 to 78
189 (near infrared (NIR)) and 221-242 (shortwave infrared (SWIR)). Additionally, the 45
190 bands strongly affected by water absorption and noise were removed leaving a
191 Hyperion data cube comprising 146 wavebands (Table 1).

192

Table 1. Selected usable bands of Hyperion image

Range (nm)	488-925	933	973-1114	1155-1336	1477-1790	1981-1991	2032-2355	Total
Bands	14-57	79	83-97	101-119	133-164	183-184	188-220	146 usable bands

193

194

195

196

197

198

199

200

201

202

203

204

205

206

207

208

209

210

211

212

The FLAASH atmospheric correction (ENVI 4.4) routine was applied to the data cube to remove the effects of the atmosphere and transform the raw radiance data ($Wm^{-2} sr^{-1}\mu m^{-1}$) to rescaled reflectance (%). Hyperion images provide effective measures of reflectance from the Earth surface if “smile effect” and random noise are managed. The “smile effect” refers to an across-track wavelength shift from the central wavelength, due to a change of dispersion angle with field position. In VNIR bands the shift range is between 2.6- to 3.5 nm, with the maximum shift occurring at column 256 in band 10. In SWIR bands, the spectral shift is less than 1 nm and is not significant for forest applications (Goodenough et al. 2003). The smile effect may affect Hyperion images in different degrees of the spectral range and may vary from scene to scene. Thus two methods developed by Dadon et al (2010) were employed to detect the smile effect in the Hyperion data cube. The first method uses the effects of the gas absorption features of O₂ around 760 nm (VNIR) and 2012 nm (SWIR) and the second method applies the Minimum Noise Fraction (MNF) transformation where the band MNF-1 showed a strong spatial gradient corresponding to the spectral smile. Subsequently, the “smile effect” was successfully removed by applying the approach developed by Datt et al (2003). This method relies in the significantly modified gain and offset values of columns affected by vertical stripes, therefore the statistical moments for each column are modified to match those for the whole image for each Hyperion band.

$$X'_{ijk} = \alpha_{ik} \cdot X_{ijk} + \beta_{ik} \quad (1.1)$$

213

Gains and offsets are computed by:

$$\alpha_{ik} = \frac{\bar{S}_{ik}}{S_{ik}} \quad (1.2)$$

$$\beta_{ik} = \bar{m}_{ik} - \alpha_{ik} \cdot m_{ik} \quad (1.3)$$

214 Where:

215 m_{ik} = mean of the detector at i th column for band k .

216 \bar{m}_{ik} = mean reference value.

217 S_{ik} = within column standard deviation.

218 \bar{S}_{ik} = within column standard deviation reference value.

219

220 The method takes into account the reference mean to be the total image mean and the
221 reference standard deviation to be the whole image within column standard deviation.

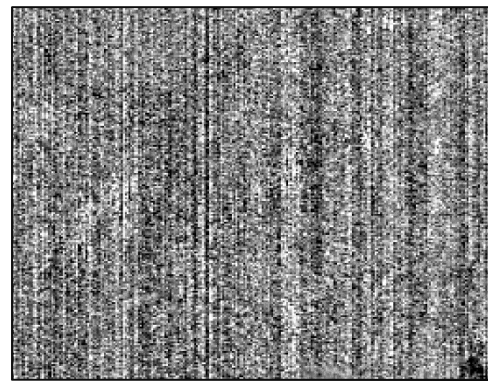
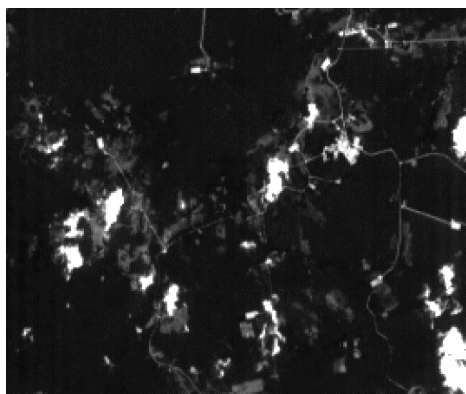
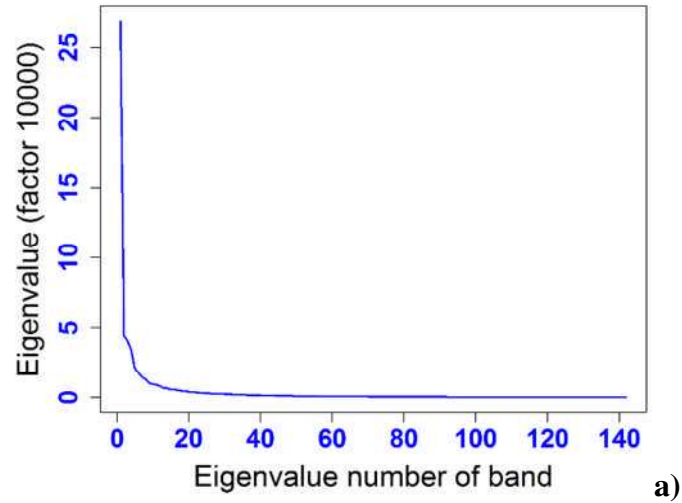
$$\bar{m}_{ik} = \bar{m}_k \quad (1.4)$$

$$\bar{S}_{ik} = \bar{S}_k \quad (1.5)$$

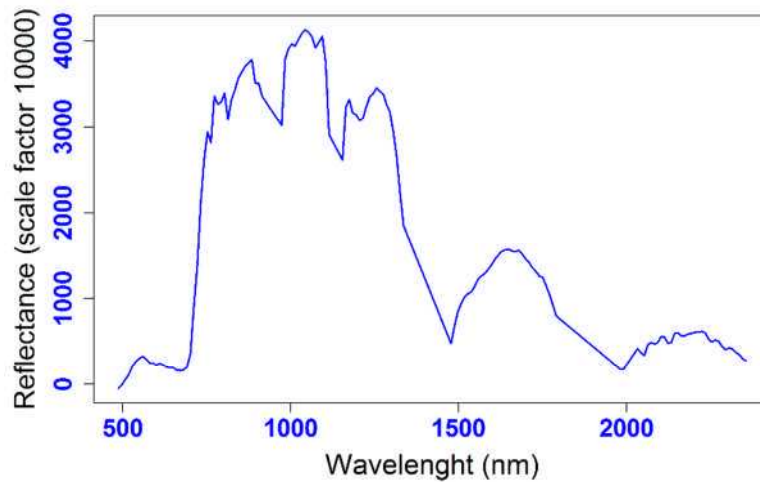
222

223 Noise reduction: Finally, the MNF (Minimum Noise Fraction) method was
224 applied to reduce noise and data dimensionality. MNF is an algorithm used for ordering
225 data cubes into components of image quality using a two-cascade-principal-
226 components-transform which selects new components in order to decreasing signal to
227 noise ratio (SNR) (Goodenough et al. 2011, Apan et al. 2004). In this study, forward
228 MNF transformation was applied to the 146 usable bands of Hyperion cube and the
229 result shown in Figure 2a illustrates that most of the information (83%) is contained in
230 the first 15 MNF bands represented by the higher eigenvalues. Figure 2b shows the first
231 MNF band which contains most of the information (43.6%) and Figure 2c illustrates
232 that MNF band 15 contains noise and little information. MNF bands between 16 and
233 146 basically contain noise (Datt et al. 2003). The next step was to apply the inverse
234 MNF process to the 15 bands containing useful information in order to transform back
235 to the 146 Hyperion spectral bands removing in this way the low SNR from the data.

236 Figure 3Error! Reference source not found. illustrates the Hyperion spectral signal
237 after pre-processing steps.
238



239 Figure 2. a) Eigenvalues for the 146 Hyperion spectral bands; b) MNF Band 1
240 containing most of the information (44%); c) MNF band 15 (0.9)
241



242
243 Figure 3. Resulting Hyperion spectral signal after pre-processing

244 **2.4. Spectral vegetation indices (VI)**

245 Several VI grouped in broad-band, narrow-band-greenness/chlorophyll, narrow-band-
246 other pigments and narrow-band-water indices were computed (Table 2 and Annex 4 in
247 Supplementary Materials) from the processed Hyperion data. From them, a total of 28
248 indices were selected. Some indices, like PRI (Photochemical Reflectance Index)
249 (Gamon;Peñuelas & Field 1992) and CARTER 1 (Carter 1994) did not resolve
250 appropriately when applied to our Hyperion data. Most of the non-applicable indices
251 used reflectance values in the blue range of the spectrum where Hyperion data showed
252 low SNR.

253 A value for every pixel covering each of the study sites was extracted for each
254 vegetation index (in total Site 1 covers 18000 m² (20 pixels); Site 2 covers 14000 m²
255 (16 pixels) and Site 3, 64800 m² (72 pixels)).

256

257

258

259

260

Table 2. Vegetation indices applied to Hyperion images in the study area

	INDEX	EQUATION	REFERENCES
BROAD-BAND INDICES			
1	Simple Ratio (SR)	$\frac{\rho_{NIR}}{\rho_{Red}}$	(Rouse;Haas & Schell 1974)
2	Normalised Difference Vegetation Index (NDVI)	$\frac{\rho_{NIR} - \rho_{Red}}{\rho_{NIR} + \rho_{Red}}$	(Rouse;Haas & Schell 1974)
3	Green Normalised Difference Vegetation Index (GNDVI)	$\frac{\rho_{NIR} - \rho_{Green}}{\rho_{NIR} + \rho_{Green}}$	(Gitelson;Kaufman & Merzlyak 1996)
4	Enhanced Vegetation Index (EVI)	$2.5 \frac{\rho_{NIR} - \rho_{Red}}{\rho_{NIR} + 6\rho_{Red} - 7.5\rho_{Blue} + 1}$	(Huete et al. 1997)
5	Atmospherically Resistant Vegetation Index (ARVI)	$\frac{\rho_{NIR} - (2\rho_{Red} - \rho_{Blue})}{\rho_{NIR} + (2\rho_{Red} - \rho_{Blue})}$	(Kaufman&Tanre 1992)
NARROW-BAND INDICES: GREENES, CHLOROPHYLL, REP			
6	Sum Green (SG)	$\sum_{600nm}^{500nm} \rho_{Green}$	(Gamon&Surfus 1999)
7	Pigment Specific Simple Ratio-Chl (PSSRa)	$\frac{\rho_{800}}{\rho_{680}}$	(Blackburn 1998)()
8	Red-Edge Normalised Difference Index (NDVI ₇₀₅)	$\frac{\rho_{750} - \rho_{705}}{\rho_{750} + \rho_{705}}$	(Sims&Gamon 2002)
9	Modified Red-Edge Simple Ratio (mSR ₇₀₅)	$\frac{\rho_{750} - \rho_{445}}{\rho_{705} + \rho_{445}}$	(Sims&Gamon 2002)
10	Modified Red-Edge Normalised Difference Index (mNDVI ₇₀₅)	$\frac{\rho_{750} - \rho_{705}}{\rho_{750} + \rho_{705} + 2\rho_{445}}$	(Sims&Gamon 2002)
11	Carter Index 2 (CTR2)	$\frac{\rho_{695}}{\rho_{760}}$	(Carter;Cibula & Miller 1996)
12	Lichtenthaler Index 1(LIC1) or Pigment Specific Normalised Difference – Chla (PSNDa)	$\frac{\rho_{800} - \rho_{680}}{\rho_{800} + \rho_{680}}$	(Blackburn 1998, Lichtenthaler et al. 1996)
13	Optimised Soil-Adjusted Vegetation Index (OSAVI)	$1 + 0.16 \frac{\rho_{800} - \rho_{670}}{\rho_{800} - \rho_{670} + 0.16}$	(Rondeaux;Steven & Baret 1996)
14	Modified Chlorophyll Absorption Ratio Index (MCARI)	$\frac{\rho_{700}}{\rho_{670}}[(\rho_{700} - \rho_{670}) - 0.2(\rho_{700} - \rho_{550})]$	(Daughtry et al. 2000)
15	Ratio of derivatives at 725 and 702 nm (Der ₇₂₅₋₇₀₂)	$\frac{d\rho/d\lambda_{725}}{d\rho/d\lambda_{702}}$	(Smith;Steven & Colls 2004)
16	Red-Edge Position (REP)	$\rho_{re} = \frac{\rho_{670} + \rho_{780}}{2}$ $700 + 40 \frac{\rho_{re} - \rho_{700}}{\rho_{740} - \rho_{700}}$	(Guyot;Baret & Major 1988)
17	Vogelmann Red-Edge Index (VOG1)	$\frac{\rho_{740}}{\rho_{720}}$	(Vogelmann;Rock & Moss 1993)
18	Chlorophyll Index (CI ₅₉₀)	$\frac{\rho_{880}}{\rho_{590}} - 1$	(Gitelson&Merzlyak 1997)
19	MERIS Terrestrial Chlorophyll Index (MTCI)	$\frac{\rho_{753.75} - \rho_{708.75}}{\rho_{708.75} - \rho_{681.25}}$	(Curran&Dash 2005)

NARROW-BAND INDICES: OTHER PIGMENTS			
20	Structure Insensitive Pigment Index (SIPI)	$\frac{\rho_{800} - \rho_{445}}{\rho_{800} - \rho_{680}}$	(Peñuelas et al. 1995)
21	Red Green Ratio (RG)	$\frac{\sum \rho_{Red}}{\sum \rho_{Green}}$	(Gamon&Surfus 1999)
22	Anthocyanin Reflectance Index 1 (ARI1)	$\frac{1}{\rho_{550}} - \frac{1}{\rho_{700}}$	(Gitelson;Merzlyak & Chivkunova 2001)(^o)
23	Anthocyanin Reflectance Index 2 (ARI2)	$\rho_{800} \left[\frac{1}{\rho_{550}} - \frac{1}{\rho_{700}} \right]$	(Gitelson;Merzlyak & Chivkunova 2001)
NARROW BAND INDICES: WATER			
24	Water Band Index (WBI)	$\frac{\rho_{900}}{\rho_{970}}$	(Peñuelas et al. 1997)
25	Normalised Difference Water Index (NDWI)	$\frac{\rho_{857} - \rho_{1241}}{\rho_{857} + \rho_{1241}}$	(Gao 1996)
26	Moisture Stress Index (MSI)	$\frac{\rho_{1599}}{\rho_{819}}$	(Hunt Jr&Rock 1989)
27	Normalised Difference Infrared Index (NDII)	$\frac{\rho_{819} - \rho_{1649}}{\rho_{819} + \rho_{1649}}$	(Hardisky;Klema & Smart 1983)
28	Normalised Heading Index (NHI)	$\frac{\rho_{1100} - \rho_{1200}}{\rho_{1100} + \rho_{1200}}$	(Pimstein et al. 2009)

262 **2.5. Data analysis**

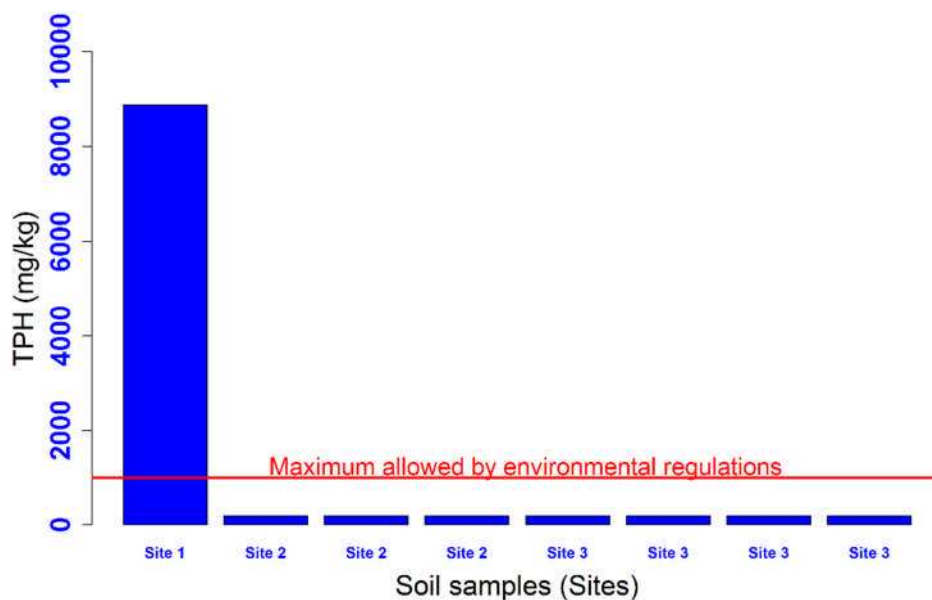
263 The mean and standard deviation was calculated for all data generated for each
264 site (both field- and imagery-based). To assess whether there has been any oil pollution
265 on the forest it is expected that there will be a statistically significant difference in the
266 levels of contaminant in the soil between the sites and that being so, any corresponding
267 statistical difference present in the vegetation indices could ultimately be used to
268 determine pollution from space and presented as a map of contamination. This
269 difference was determined using an ANOVA. Those vegetation indices exhibiting a
270 significant difference in the ANOVA at 99.9% confidence level (p<0.001) were then
271 used in a post-hoc pairwise comparison using the adjustment method of Holm (see
272 Table 4) to determine the pairwise significant differences between sites. Those indices
273 exhibiting strongly significant differences between sites were used to map an area of 52
274 km² which covered a petroleum production region. A threshold was determined for each

275 of the selected vegetation indices based on the median and the min/max value which
276 better characterises the area affected by oil pollution. Based on the threshold values, a
277 mask was created for each vegetation index. An image of vegetation contamination was
278 computed by summing the masks such that a pixel value having the value that equalled
279 the sum of the number of vegetation indices used is one containing contaminated forest.

280 3. Results

281 3.1. Analysis of field-derived data

282 The results of the soil analysis (presented in Annex 1-Supplementary Materials)
283 showed that Site 1 (polluted) had high levels of Total Petroleum Hydrocarbon (TPHs),
284 near 9000 mg/kg. All the soils sampled at Sites 2 (non-polluted) and Site 3 (Pristine
285 forest-Yasuni) reported values lower than 200 mg/kg which confirms that these two
286 sites were not affected by hydrocarbons pollution (Figure 4).



287 Figure 4. Results of TPHs (Total Petroleum Hydrocarbons) for the study sites compared
288 with the environmental regulation threshold established by the Environmental Ministry
289 of Ecuador.
290

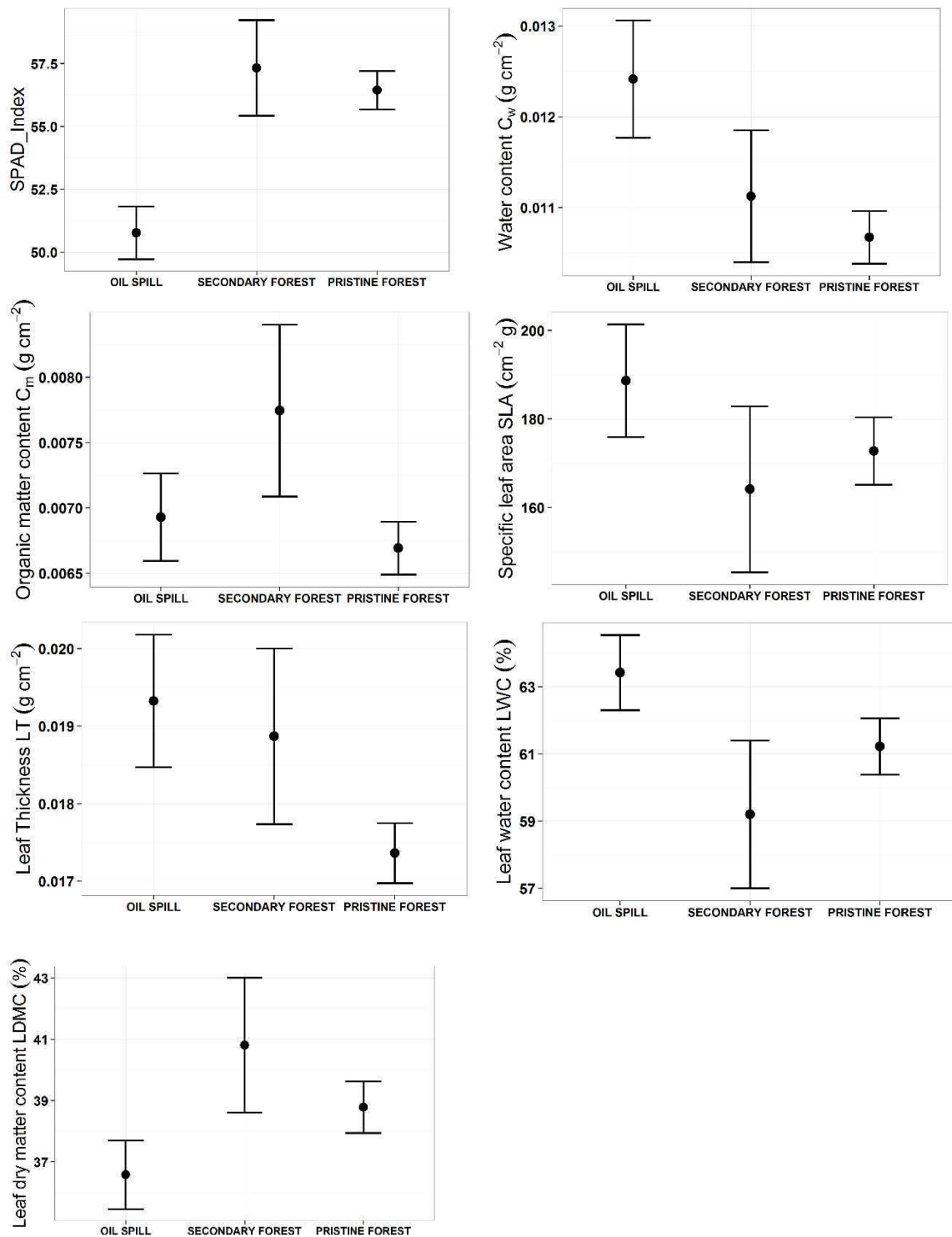
291 **3.2. Analysis of foliar biophysical and biochemical parameters**

292 Initial focus on the plotted means and $\pm 95\%$ confidence intervals for each foliar
293 biochemical/biophysical variable (Figure 5. Mean and $\pm 95\%$ confidence interval for the
294 foliar biophysical and biochemical parameters

295 ; descriptive statistics presented in Annex 5 of Supplementary Materials), and
296 the ANOVA and associated pairwise comparisons via the Holm method (Table 3), was
297 on how different site 1 (polluted) was from sites 2 and 3. The chlorophyll content (C_{ab})
298 was significantly lower at site 1 with values strongly different (99.9%) to those for the
299 two non-polluted sites (2 and 3). No significant difference in chlorophyll content was
300 evident between the two unpolluted sites. Leaf water content (LWC) and Leaf dry
301 matter content ($LDMC$) also exhibited strongly significant differences (99.9%) between
302 the unpolluted site 1 and sites 2 (strongly significant at 99.9%) and 3 (highly significant
303 at 99%). Total water content (C_w) difference however had a slightly different pattern
304 with differences observed between site 1 and 2 only significant at 95% level but highly
305 significant (at 99.9%) between site 1 and site 3.

306 Organic matter content (C_m) was significantly different (95%) between Site 1
307 and 2 but insignificant in difference between Site 1 and 3, with a high (99%) level of
308 significance difference being shown between the two unpolluted sites. Leaf thickness
309 (Lt) was strongly significantly different (99.9%) between Site 1 and 3 but no difference
310 was observed between Sites 1 and 2 for this foliar property. No differences in SLA were
311 observed between any of the sites.

312



313 Figure 5. Mean and $\pm 95\%$ confidence interval for the foliar biophysical and biochemical
 314 parameters
 315

316 Table 3. Pairwise comparison of p-values with holm adjustment method

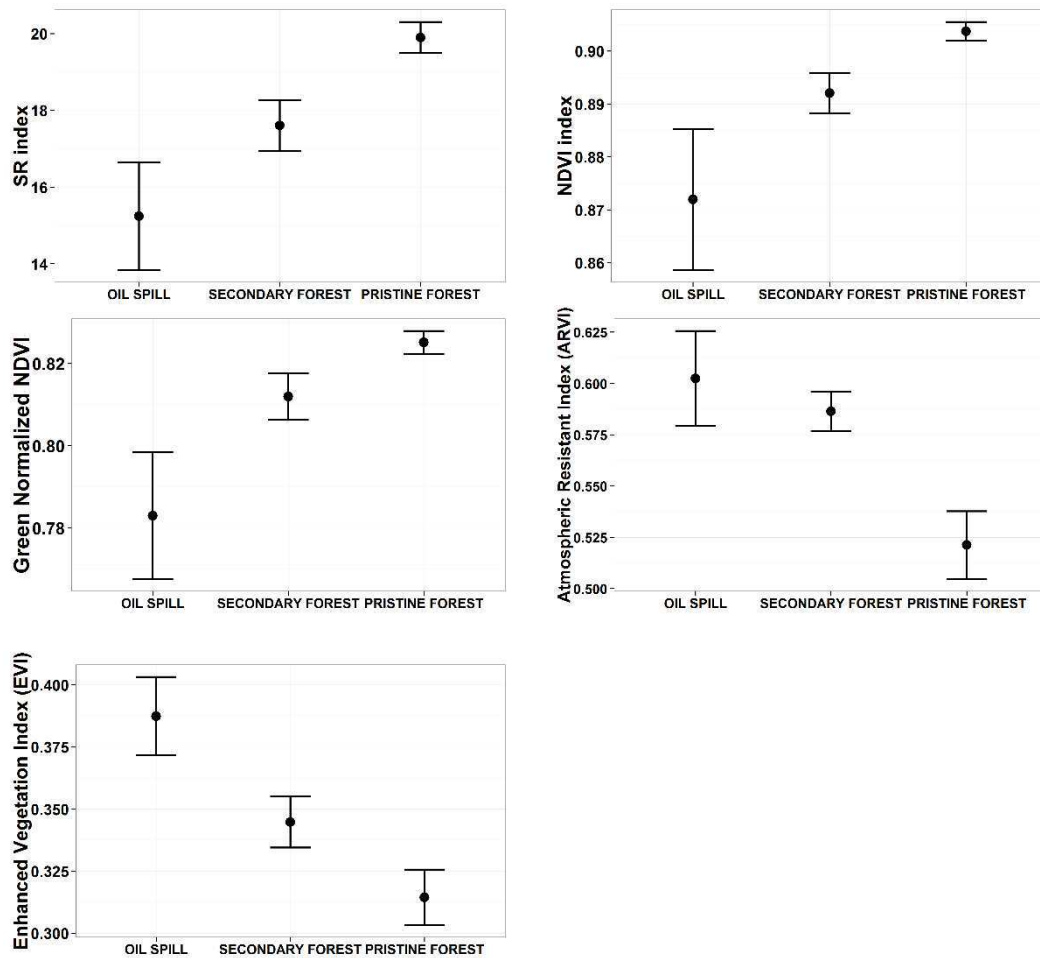
	C_{ab}	C_w	C_m	SLA	L_t	LWC	$LDMC$
ANOVA test	2.0E-16	4.2E-07	1.7E-03	2.8E-02	2.2E-05	1.5E-05	1.5E-04
	***	***	**	*	***	***	***

Pairwise comparison – Holm adjustment method							
Oil spill (Site 1)- No Polluted (Site 2)	6.2E-10 ***	2.1E-02 *	1.5E-02 *	7.8E-02	5.0E-01	4.4E-04 ***	4.4E-04 ***
Oil spill (Site 1)- Pristine forest (Site 3)	1.2E-14 ***	2.2E-07 ***	2.3E-01	7.8E-02	2.0E-05 ***	4.2E-03 **	4.2E-03 **
No polluted (Site 2)- Pristine forest (Site 3)	2.1E-01	3.5E-01	1.1E-03 **	4.2E-01	4.3E-02 *	5.8E-02	5.8E-02
*** Strongly significant (99.9%) ** Highly significant (99%) * Significant (95%) No significant difference							

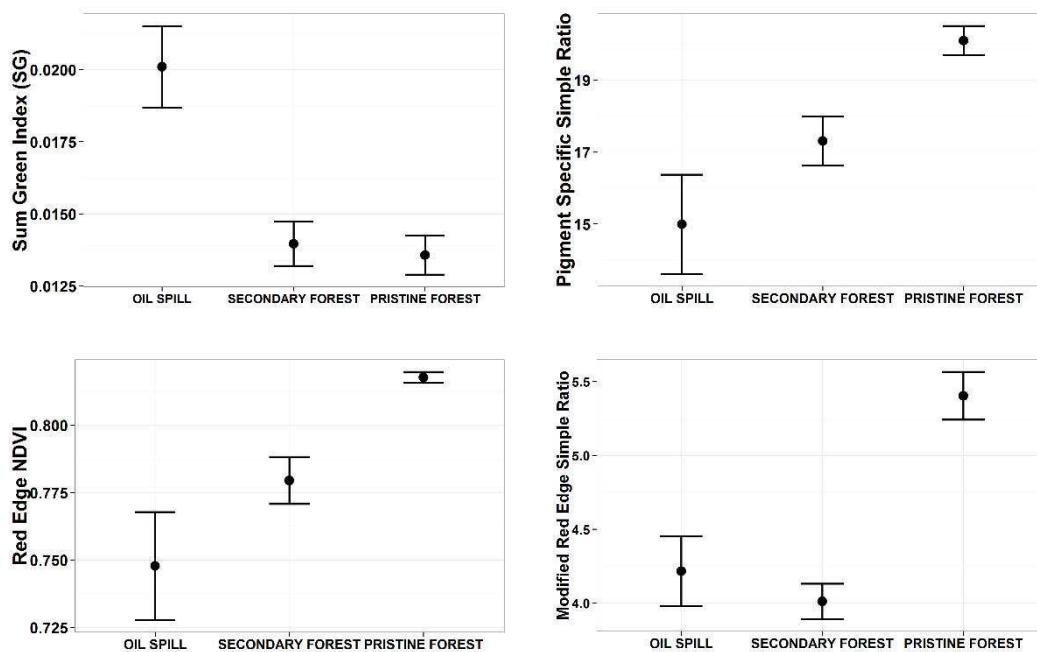
317 **3.3. Analysis of vegetation indices from Hyperion images**

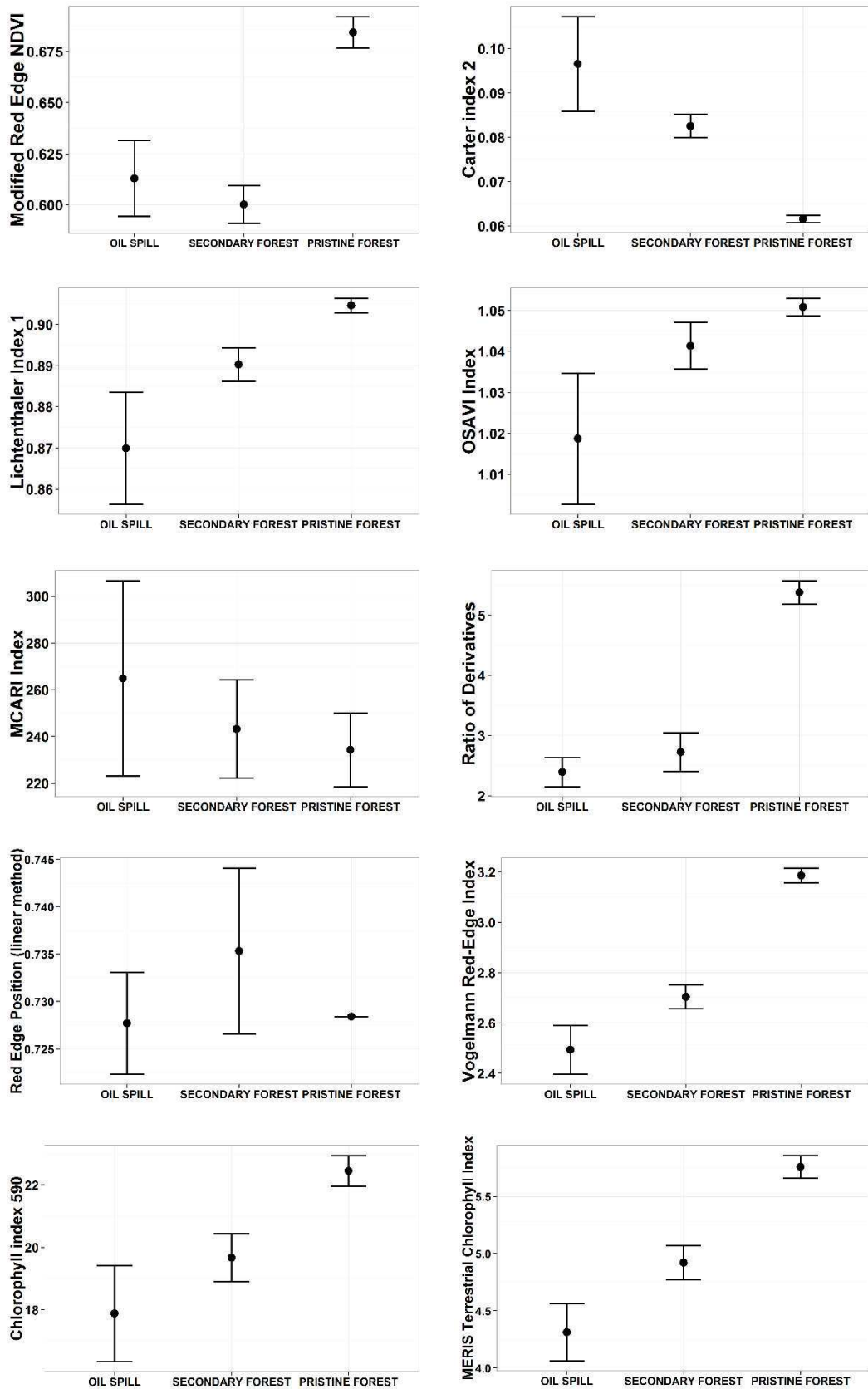
318 Means and standard deviations obtained for each set of vegetation indices are
319 shown in Figure 6 (broadband), Figure 7 (greenness, chlorophyll, REP), Figure 8 (other
320 pigments) and Figure 9 (water indices). The corresponding pairwise comparisons via
321 the Holm method are presented in Table 4.

322 Most vegetation indices (23 of the 28) illustrated 99.9% significance difference
323 between Site 1 (polluted) and Site 3 (pristine forest) which are the most dissimilar sites
324 in terms of forest structure, plant species and conservation. 16 of 28 indices showed
325 99.9% significance differences between Site 2 (secondary non-polluted forest) and Site
326 3 (pristine forest) and just 11 vegetation indices registered 99.9% significance between
327 Site 1 (polluted) and Site 2 (non-polluted forest). Of those 11 vegetation indices which
328 were able to discriminate as strongly significant (99.9%) the difference between the two
329 sampled secondary forests (Site 1 and Site 2), all of them corresponding to broad-band
330 indices and narrow-band-greenness-chlorophyll-red-edge index groups. Lower and no-
331 significance were found in indices grouped under other pigments and water indices.
332 Annex 6, Annex 7 and Annex 8 in the Supplementary Material section present the
333 descriptive statistics for each vegetation index applied and for each study site.

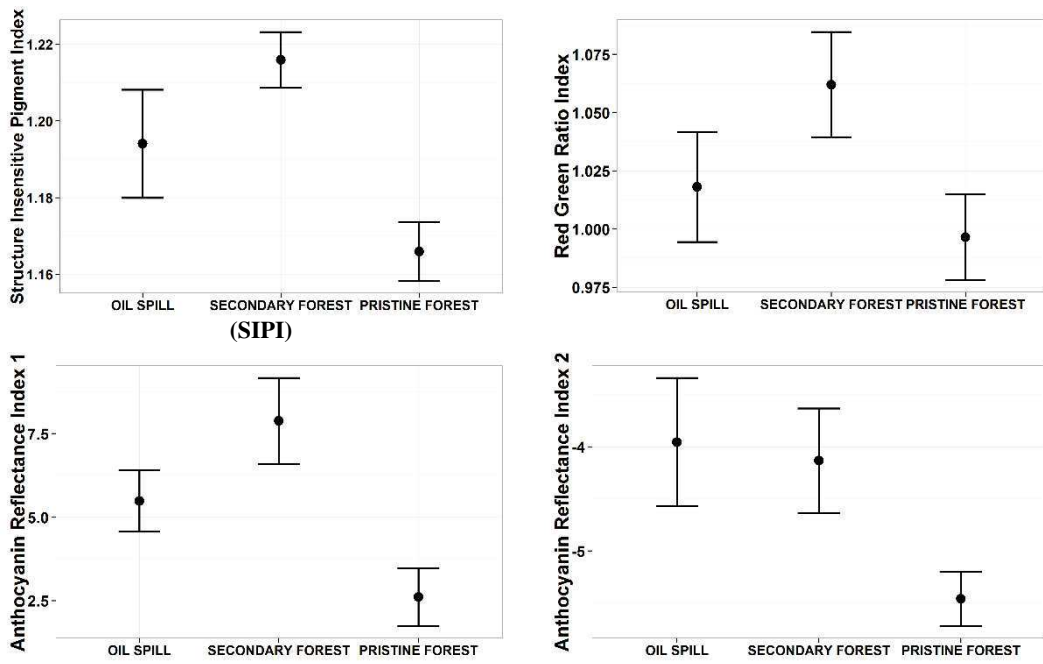


334 Figure 6. Mean and $\pm 95\%$ confidence interval of the calculated Broad-band vegetation
 335 indices

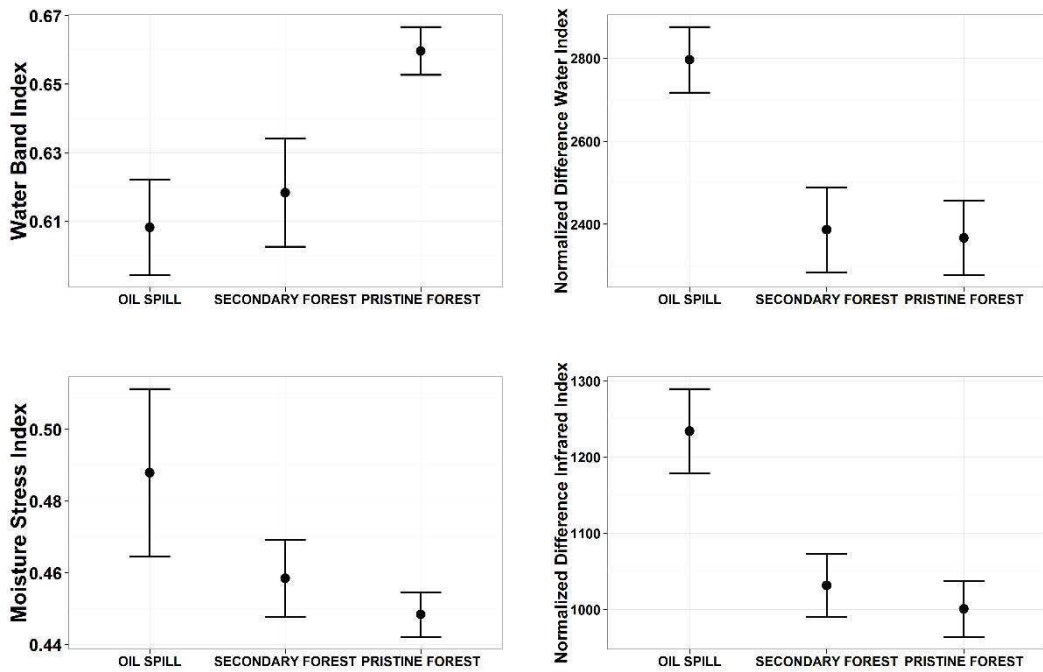


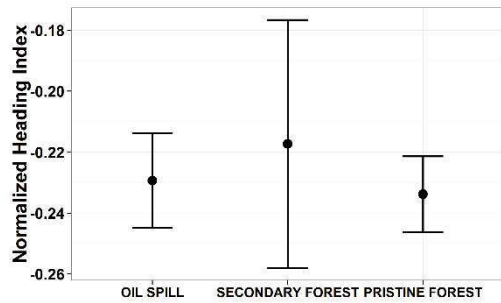


336 Figure 7. Mean and $\pm 95\%$ confidence interval of the calculated Narrow-Band
 337 Vegetation Indices: Greenness / Chlorophyll indices
 338



340 Figure 8. Mean and $\pm 95\%$ confidence interval of the calculated Narrow-Band
 341 Vegetation Indices: Other pigments
 342





343 Figure 9. Mean and $\pm 95\%$ confidence interval of the calculated Narrow-Band
 344 Vegetation Indices: Water Indices
 345

346 Table 4. Analysis of variance and pairwise comparison of means using Holm
 347 adjustment method for the study sites (oil pollution, secondary forest and pristine forest)

	INDEX	Site 1 (polluted) vs. Site 2 (non- polluted)	Site 1 (polluted) vs. Site 3 (pristine forest)	Site 2 (non- polluted) vs. Site 3 (pristine forest)
BROAD-BAND VEGETATION INDICES				
1	SR	***	***	***
2	NDVI	***	***	**
3	GNDVI	***	***	**
4	ARVI	ns	***	***
5	EVI	**	***	*
NARROW-BAND VEGETATION INDICES				
GREENNESS / CHLOROPHYLL				
6	SG	***	***	ns
7	PSSRa	***	***	***
8	NDVI ₇₀₅	***	***	***
9	mSR ₇₀₅	ns	***	***
10	mNDVI ₇₀₅	ns	***	***
11	CRT2	***	***	***
12	LIC1 or PSNDa	***	***	**
13	OSAVI	***	***	*
14	MCARI	ns	ns	ns
15	Der ₇₂₅₋₇₀₂	ns	***	***
16	REP	**	ns	**
17	VOG1	***	***	***
18	CI ₅₉₀	*	***	***
19	MTCI	***	***	***
OTHER PIGMENTS				
20	SIPI	*	***	***
21	RG	ns	ns	**
22	ARI1	*	**	***
23	ARI2	ns	***	***
WATER INDICES				
24	WBI	ns	***	***
25	NDWI	.	***	*
26	MSI	*	***	ns

27	NDII	ns	***	***
28	NHI	ns	ns	ns
*** Strongly significant (0.1%) ** Highly significant (1%) * Significant (5%) . Lowest significant (10%) ns No significant				

348

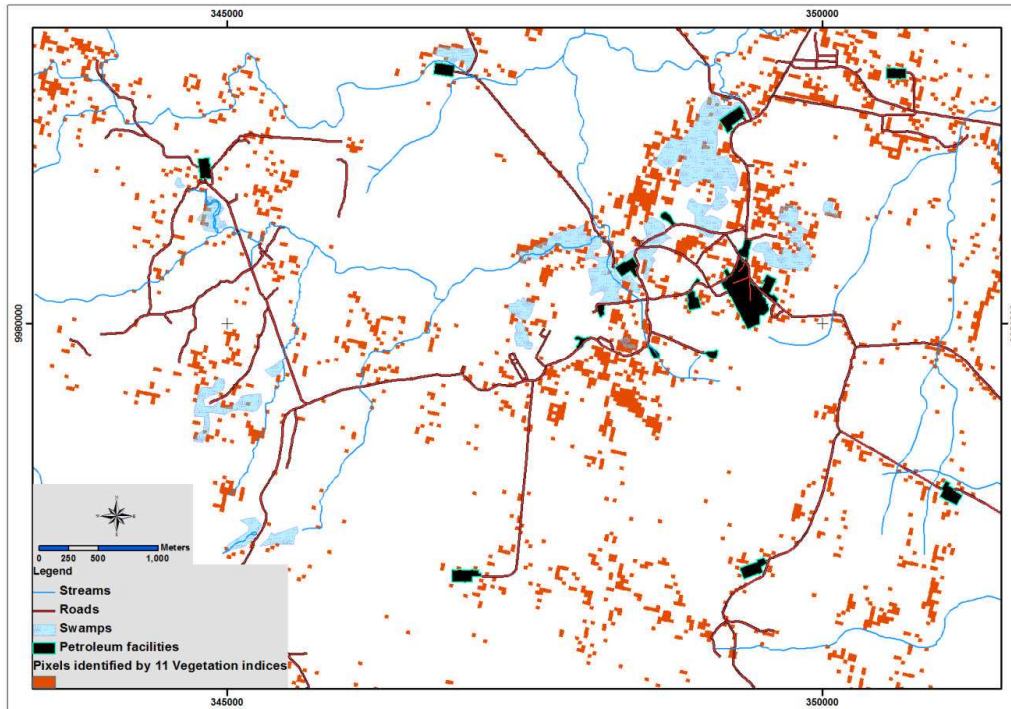
349 **3.4. Mapping vegetation stress**

350 The eleven vegetation indices that strongly discriminated polluted and non-
351 polluted secondary forests (strongly significant at 0.1% level of confidence - see Table
352 **4**) were selected as the more sensitive indices to detect the effects of petroleum
353 pollution. Thresholds were defined based on the median and the min/max values of the
354 oil spill site (see Table 5 and Supplementary Materials, Annex 9). Based on those
355 thresholds, a map (Figure 10) illustrate the locations of contaminated forest was
356 produced (effect). Also mapped is the infrastructure for petroleum extraction: platforms,
357 stations, oil pipelines and roads (cause). In the majority of cases the cause and effect are
358 spatially coincident.

359
360
361

Table 5. Threshold values defined for selected vegetation indices in the site affected by hydrocarbon pollution

Index	Median	Min/Max value
SR	16.3065	8.5502 (min.)
NDVI	0.8844	0.7906 (min.)
GNDVI	0.7987	0.7096 (min.)
SG	0.0193	0.0278 (max.)
PSSRa	16.0014	8.3391 (min.)
NDVI ₇₀₅	0.7620	0.6351 (min.)
CTR2	0.08669	0.1603 (max.)
LIC1	0.8844	0.7906 (min.)
OSAVI	1.0290	0.9284 (min.)
VOG1	2.5724	2.0433 (min.)
MTCI	4.4889	3.0824 (min.)



362
 363 Figure 10. Areas identified as vegetation stress based on the eleven vegetation indices.
 364

365 To ascertain the importance of each the 11 VI in the mapping of contamination a
 366 discriminant function analysis was undertaken which illustrates that three VI (the SG,
 367 NDVI and NDVI₇₀₅) explain 83% of the ability to separate between the 3 sites (Table
 368 6). Figure 11 remaps contamination based on these 3 VI only showing a close
 369 agreement with Figure 10. By way of validation Figure 12 depicts those sites sampled
 370 in the field that have been correctly allocated as either contaminated or uncontaminated.
 371 This Figure also affords closer examination of the cause and effect of the hydrocarbon
 372 contamination in these forests.

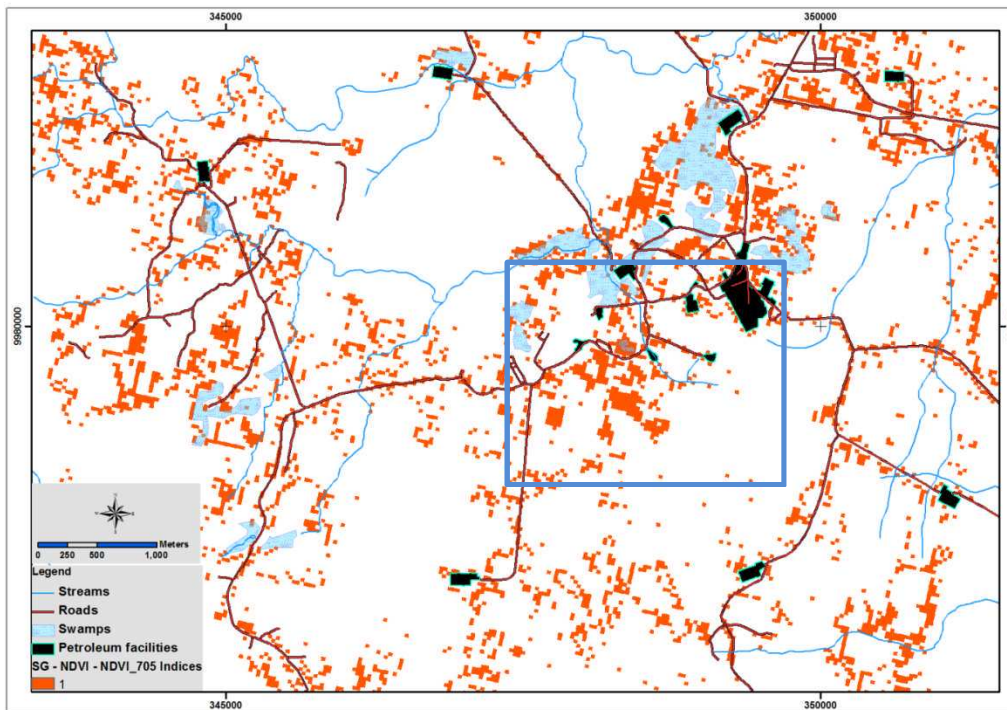
373

Table 6. Results of discrimination function analysis

Vegetation indices	LD1	LD2	Relative weight (LD1)
SG	592.0	-735.9	53.0%
NDVI	-241.2	115.5	21.6%
NDVI ₇₀₅	94.1	18.7	8.4%
CTR2	51.7	-23.7	4.6%
GNDVI	-51.1	-146.7	4.6%
LIC1	39.3	5.9	3.5%
VOG1	27.4	24.5	2.4%

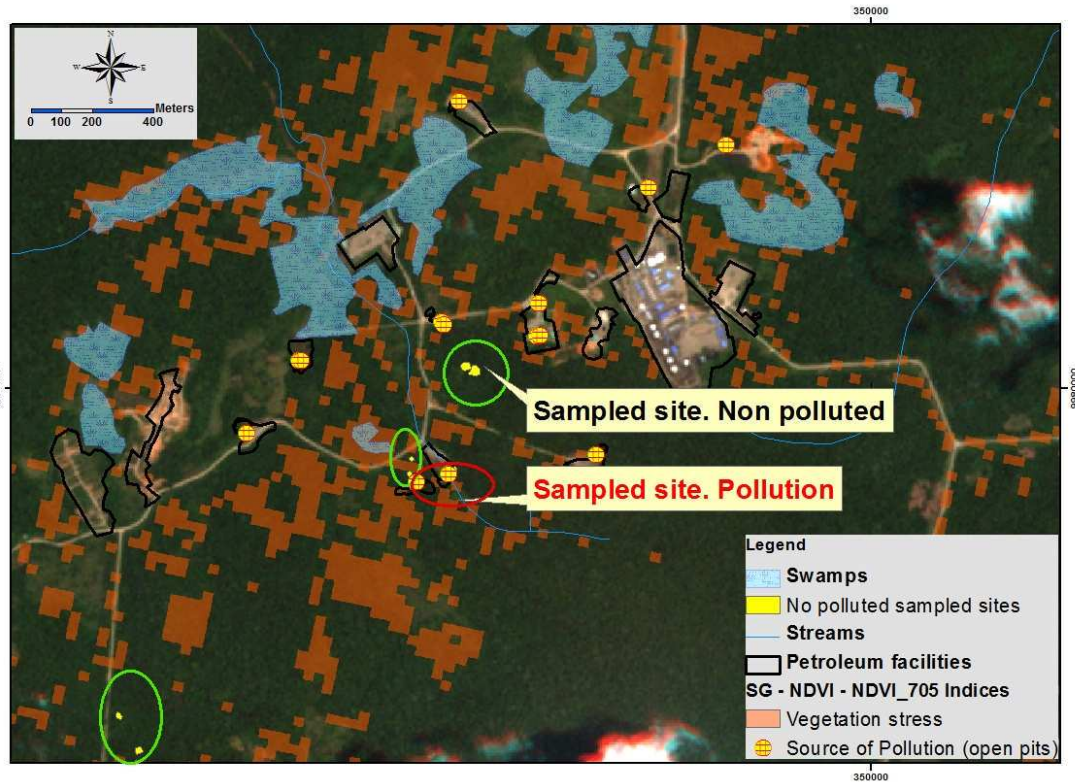
OSAVI	-9.8	-22.6	0.9%
MTCI	-3.7	-4.8	0.3%
PSSRa	3.5	1.9	0.3%
SR	-2.6	-3.2	0.2%
Trace proportion (variance)	95.0%	5.0%	
Eigenvalues	69.3	16.0	
	between	within sites	

374



375
376
377
378
379

Figure 11. Areas identified as vegetation stress based on the SG, NDVI and NDVI_705 indices which together contribute to 83% of the site separability. The blue square is that highlighted in Figure 10.



380
 381 Figure 12. Areas detected as vegetation stress in petroleum productive area. Open pits
 382 identified as source of pollution and RAPIDEYE images (background) have been
 383 provided by the Environmental Ministry of Ecuador (PRAS-program)

384 4. Discussion

385 4.1. Petroleum contamination in soil

386 The soil analyses of this study revealed a latent effect of the formerly disposed
 387 hydrocarbons at Site 1. Since the environmental regulations in Ecuador state the
 388 maximum level of TPHs for sensible ecosystems to be 1000 mg/kg (Ministerio de
 389 Energia y Minas 2001) it is clear that this site is affected by petroleum pollution. Other
 390 sources of pollution identified as open pits and facilities where polluted soils have been
 391 stocked for remediation have been identified by environment audits and studies carried
 392 out by the Environmental Ministry of Ecuador (Environmental Ministry of Ecuador
 393 2014). At those sites crude oil has been exposed to the environment and although lighter
 394 hydrocarbons (gaseous) have evaporated and biodegraded, liquid hydrocarbons have
 395 migrated from the open pits by infiltration into the soil and dissolution in water

396 (Environmental Ministry of Ecuador 2005, Environmental Ministry of Ecuador 2009).
397 Any vegetation in close proximity has thus potential to be impacted. Water transports
398 pollutants away from its source, which are subsequently deposited in the nearby
399 swamps to accumulate. This also impacts on the vegetation. This was particularly
400 evident in Figure 10 and Figure 12 where a cluster of pixels identified as stressed
401 vegetation is located around swamps. As expected, sites 2 and 3 had no soil
402 contamination, being located away from sources of petroleum production.

403 ***4.2. Impact of petroleum contamination on leaf properties***

404 Of the leaf biochemical and biophysical properties measured it was chlorophyll
405 content and those associated with water content that exhibited significant differences
406 between the polluted site and non-polluted sites. The low levels of chlorophyll content
407 seen at site 1 indicate vegetation stress caused by a reduction of photosynthetic activity
408 in vegetation exposed to petroleum contaminant. The C_{ab} content is responsive to a
409 range of stresses on vegetation because of its direct role in the photosynthetic processes
410 of light harvesting and initiation of electron transport (Zarco-Tejada et al. 2000). The
411 higher values of water content (C_w) observed at the polluted site may be linked to the
412 adaptation process of plants to close the stomata under stress conditions as strategy to
413 reduce transpiration, which in turns reduce photosynthetic rate linked to the lower
414 chlorophyll and thus total tree metabolism (Larcher 2003, Zweifel; Rigling & Dobbertin
415 2009). Other foliar properties related to water, those expressed on mass basis (% LWC
416 and % LDMC) also differed and is due to the fact that as these parameters are not
417 normalised by the leaf area, these differences can be explained by the high species
418 diversity of the sample sites where leaves vary greatly in morphology, anatomy and
419 physiology in response to their growing conditions (Tedersoo et al. 2010). Of these leaf
420 variables, it is chlorophyll content that lends itself to be measured from space using a

421 hyperspectral sensor, and since it is this that showed differences between the polluted
422 and unpolluted sites, this suggests that by measuring this biochemical in vegetation
423 compartments, detection of petroleum contamination across vast expanse of tropical
424 forests is indeed possible.

425 Other studies have suggested leaf thickness to be a useful indicator of vegetation
426 stress. Either as a result of increased levels of foliar water content per unit area and/or a
427 shift of species composition. Indeed, some species may be replaced by invasive species
428 which are more resistant to the petroleum influence (Noomen;van der Werff & van der
429 Meer 2012). However, here leaf thickness showed no significant difference between the
430 oil spill secondary and non-oil spill secondary so this is inconclusive and not a clear
431 variable to measure from space.

432 ***4.3. Vegetation indices to detect the occurrence of petroleum pollution***

433 As suggested by the field data it was those vegetation indices with sensitivity to
434 photosynthetic pigments that were most useful in discriminating between the
435 contaminated and non-contaminated sites. The Sum Green vegetation index (SG)
436 clearly identified an increased reflectance signal in the visible spectral region of the area
437 affected by petroleum pollution which confirms the sensitivity of Hyperion image to
438 register reduced chlorophyll content levels in the polluted site. Also of use are the
439 broad-band and narrow-band vegetation indices related to the traditional NDVI (SR,
440 GNDVI, NDVI₇₀₅), endorsing the conclusions of (Zhu et al. 2013).

441 Two narrow-band indices developed to estimate chlorophyll content across
442 species (PSSRa and NDVI₇₀₅) clearly exhibited lower chlorophyll content for the
443 tropical forest affected by petroleum. However, this contradicts Sims and Gamon's
444 (2002) conclusions which suggested that PSSRa was largely insensitive to variations in
445 chlorophyll content in a multispecies forest. Conversely, this study agrees with their

446 findings related to the sensitive of NDVI₇₀₅ to variations of chlorophyll content across
447 several species. The narrow-band indices NDVI₇₀₅, CTR2, LIC1 and OSAVI also
448 showed strong significant differences between sites, concurring with those who used
449 these indices for detecting vegetation impacted by natural hydrocarbon gases leakage
450 (Noomen&Skidmore 2009). VOG1 and MTCI indices explore the relationship between
451 REP and foliar chlorophyll content also clearly identified forest affected by
452 hydrocarbons.

453 Not all indices sensitive to photosynthetic pigments were useful – MCARI index
454 showed insensitive to chlorophyll content across multiple species. REP indices did not
455 show a strong significant difference in polluted and non-polluted sites which contradicts
456 the findings presented in other studies (Noomen & Skidmore 2009, Yang 1999,
457 Smith;Steven & Colls 2004, Smith;Steven & Colls 2004, Yang et al. 2000). Vegetation
458 indices using the blue range (EVI, ARVI, mSR₇₀₅, mNDVI₇₀₅) were not able to
459 discriminate vegetation stress in the study sites due to the fact the low reflectance signal
460 of the Hyperion images in this range of the spectrum. Vegetation indices related to other
461 plant pigments consistently show lower values for pristine forest but they were not
462 differentiating between polluted and non-polluted secondary forest. Three water content
463 indices (NDWI, MSI and NDII) were able to detect higher levels of foliar water content
464 in the site affected by hydrocarbons (Figure 9) as field data suggested.

465 The three indices of most use for mapping (explaining 83% of separability
466 between the three sites), were the SG, NDVI and NDVI₇₀₅, and are a mixture of both
467 multispectral and hyperspectral vegetation indices. This particular selection of indices
468 seems to be based on their ability to highlight lower levels of photosynthetic pigments,
469 in particular chlorophyll (SG index) and dense vegetation with the high LAI (NDVI)
470 characteristic of tropical forest environments. To employ these indices within a

471 monitoring system to detect petroleum contamination is attractive, particularly given the
472 imminent improvements in sensor technology (e.g., launch of Sentinels) and capability
473 and the simplicity of using the spectra measured by these sensors. Although subsequent
474 studies are required to attain a greater insight into determining the relationship between
475 the key foliar biochemicals, spectral response and levels of pollutant that can be
476 detected, this is the first study to show that such a link holds promise and has been
477 enabled by the intensive fieldwork undertaken.

478 **5. Conclusions**

479 This paper provides evidence of leaf biochemical alterations in the rainforest
480 caused by petroleum pollution and demonstrates that these can be detected by
481 spaceborne satellite remote sensing. The results indicate that tropical forests exposed to
482 petroleum pollution show principally reduced levels of chlorophyll content,
483 accompanied by higher levels of foliar water content. These alterations were detectable
484 from space using the EO-1 Hyperion sensor by way of vegetation indices that are
485 sensitive to detection changes of photosynthetic activity of the forest based on
486 chlorophyll content and indices related to canopy density and vegetation vigour. This
487 investigation has shown a potential for the use of imaging spectrometers for the
488 identification and characterisation of hydrocarbon pollution or seep in dense tropical
489 forests.

490 **Acknowledgements**

491 This research has been self-funded by the corresponding author and has the support of
492 the Secretariat for Science and Technology of Ecuador (SENESCYT). We thank the
493 Environmental Ministry of Ecuador for providing environmental studies and the
494 Environmental Program for Pollution Remediation-PRAS for providing digital maps

495 and RAPID EYE satellite images of the study area. H. Balzter was supported by the
496 Royal Society Wolfson Research Merit Award, 2011/R3 and the NERC National Centre
497 for Earth Observation.

498

499 REFERENCES

- 500 Apan, A., Held, A., Phinn, S. & Markley, J. 2004, "Detecting sugarcane 'orange rust'
501 disease using EO-1 Hyperion hyperspectral imagery", *International Journal of*
502 *Remote Sensing*, vol. 25, no. 2, pp. 489-498.
- 503 Asner, G.P., Nepstad, D., Cardinot, G. & Ray, D. 2004, "Drought stress and carbon
504 uptake in an Amazon forest measured with spaceborne imaging spectroscopy",
505 *Proceedings of the National Academy of Sciences of the United States of America*,
506 vol. 101, no. 16, pp. 6039-6044.
- 507 Baker, J.M. 1970, "The effects of oil on plants", *Environmental Pollution*, vol. 1, pp.
508 27-44.
- 509 Bernal, A.M. 2011, "Power, powerlessness and petroleum: Indigenous environmental
510 claims and the limits of transnational law", *New Political Science*, vol. 33, no. 2,
511 pp. 143-167.
- 512 Blackburn, G.A. 2007, "Hyperspectral remote sensing of plant pigments", *Journal of*
513 *Experimental Botany*, vol. 58, no. 4, pp. 855-867.
- 514 Blackburn, G.A. 1998, "Spectral indices for estimating photosynthetic pigment
515 concentrations: A test using senescent tree leaves", *International Journal of Remote*
516 *Sensing*, vol. 19, no. 4, pp. 657-675.
- 517 Boyd, D.S., Entwistle, J.A., Flowers, A.G., Armitage, R.P. & Goldsmith, P.C. 2006,
518 "Remote sensing the radionuclide contaminated Belarusian landscape: A potential
519 for imaging spectrometry?", *International Journal of Remote Sensing*, vol. 27, no.
520 10, pp. 1865-1874.
- 521 Carter, G.A. 1994, "Ratios of leaf reflectances in narrow wavebands as indicators of
522 plant stress", *International Journal of Remote Sensing*, vol. 15, no. 3, pp. 697-703.
- 523 Carter, G.A., Cibula, W.G. & Miller, R.L. 1996, "Narrow-band Reflectance Imagery
524 Compared with Thermal Imagery for Early Detection of Plant Stress", *Journal of*
525 *Plant Physiology*, vol. 148, no. 5, pp. 515-522.
- 526 Curran, P.J. & Dash, J. 2005, *Algorithm theoretical basis document ATBD 2.2:*
527 *chlorophyll index*, University of Southampton, Southampton-UK.

- 528 Dadon, A., Ben-Dor, E. & Karnieli, A. 2010, "Use of Derivative Calculations and
529 Minimum Noise Fraction Transform for Detecting and Correcting the Spectral
530 Curvature Effect (Smile) in Hyperion Images", *Geoscience and Remote Sensing*,
531 *IEEE Transactions on*, vol. 48, no. 6, pp. 2603-2612.
- 532 Dash, J. & Curran, P.J. 2006, "Relationship between herbicide concentration during the
533 1960s and 1970s and the contemporary MERIS Terrestrial Chlorophyll Index
534 (MTCI) for southern Vietnam", *International Journal of Geographical Information*
535 *Science*, vol. 20, no. 8, pp. 929-939.
- 536 Datt, B. 1999, "Remote sensing of water content in Eucalyptus leaves", *Australian*
537 *Journal of Botany*, vol. 47, no. 6, pp. 909-923.
- 538 Datt, B., McVicar, T.R., Van Niel, T.G., Jupp, D.L.B. & Pearlman, J.S. 2003,
539 "Preprocessing EO-1 Hyperion hyperspectral data to support the application of
540 agricultural indexes", *IEEE Transactions on Geoscience and Remote Sensing*, vol.
541 41, no. 6 PART I, pp. 1246-1259.
- 542 Daughtry, C.S.T., Walthall, C.L., Kim, M.S., de Colstoun, E.B. & McMurtrey III, J.E.
543 2000, "Estimating Corn Leaf Chlorophyll Concentration from Leaf and Canopy
544 Reflectance", *Remote Sensing of Environment*, vol. 74, no. 2, pp. 229-239.
- 545 Davids, C. & Tyler, A.N. 2003, "Detecting contamination-induced tree stress within the
546 Chernobyl exclusion zone", *Remote Sensing of Environment*, vol. 85, no. 1, pp. 30-
547 38.
- 548 Davidson, E.A., De Araújo, A.C., Artaxo, P., Balch, J.K., Brown, I.F., C. Bustamante,
549 M.M., Coe, M.T., Defries, R.S., Keller, M., Longo, M., Munger, J.W., Schroeder,
550 W., Soares-Filho, B.S., Souza Jr., C.M. & Wofsy, S.C. 2012, "The Amazon basin
551 in transition", *Nature*, vol. 481, no. 7381, pp. 321-328.
- 552 Dawson, T.P. & Curran, P.J. 1998, "A new technique for interpolating the reflectance
553 red edge position", *International Journal of Remote Sensing*, vol. 19, no. 11, pp.
554 2133-2139.
- 555 Environmental Ministry of Ecuador 2014, *Geoinformation survey for petroleum*
556 *pollution sources*, Social and Environmental Program for Petroleum Pollution
557 Remediation-PRAS, Quito-Ecuador.
- 558 Environmental Ministry of Ecuador 2009, *Auditoria ambiental bianual de las*
559 *actividades hidrocarburíferas en el Bloque Tarapoa, campos compartidos Fanny*
560 *18B y Mariann 4A, las facilidades LTF en Lago Agrio y de cambio de operador de*
561 *ARC Ecuador Ltd., a Andes Petroleum Ecuador Ltd.*, ENTRIX, Quito-Ecuador.
- 562 Environmental Ministry of Ecuador 2005, *Auditoria ambiental externa de las*
563 *actividades hidrocarburíferas en el Bloque Tarapoa y el campo compartido Fanny*
564 *18B*, Walsh Environment Scientists and Engineers, Quito-Ecuador.
- 565 Féret, J., François, C., Gitelson, A., Asner, G.P., Barry, K.M., Panigada, C., Richardson,
566 A.D. & Jacquemoud, S. 2011, "Optimizing spectral indices and chemometric

- 567 analysis of leaf chemical properties using radiative transfer modeling", *Remote*
568 *Sensing of Environment*, vol. 115, no. 10, pp. 2742-2750.
- 569 Finer, M., Jenkins, C.N., Pimm, S.L., Keane, B. & Ross, C. 2008, "Oil and gas projects
570 in the Western Amazon: Threats to wilderness, biodiversity, and indigenous
571 peoples", *PLoS ONE*, vol. 3, no. 8.
- 572 Gamon, J.A., Peñuelas, J. & Field, C.B. 1992, "A narrow-waveband spectral index that
573 tracks diurnal changes in photosynthetic efficiency", *Remote Sensing of*
574 *Environment*, vol. 41, no. 1, pp. 35-44.
- 575 Gamon, J.A. & Surfus, J.S. 1999, "Assessing leaf pigment content and activity with a
576 reflectometer", *New Phytologist*, vol. 143, no. 1, pp. 105-117.
- 577 Gao, B.-. 1996, "NDWI - A normalized difference water index for remote sensing of
578 vegetation liquid water from space", *Remote Sensing of Environment*, vol. 58, no.
579 3, pp. 257-266.
- 580 Gerber, F., Marion, R., Olivoso, A., Jacquemoud, S., Ribeiro da Luz, B. & Fabre, S.
581 2011, "Modeling directional-hemispherical reflectance and transmittance of fresh
582 and dry leaves from 0.4 μm to 5.7 μm with the PROSPECT-VISIR model", *Remote*
583 *Sensing of Environment*, vol. 115, no. 2, pp. 404-414.
- 584 Gitelson, A.A., Kaufman, Y.J. & Merzlyak, M.N. 1996, "Use of a green channel in
585 remote sensing of global vegetation from EOS- MODIS", *Remote Sensing of*
586 *Environment*, vol. 58, no. 3, pp. 289-298.
- 587 Gitelson, A.A. & Merzlyak, M.N. 1997, "Remote estimation of chlorophyll content in
588 higher plant leaves", *International Journal of Remote Sensing*, vol. 18, no. 12, pp.
589 2691-2697.
- 590 Gitelson, A.A., Merzlyak, M.N. & Chivkunova, O.B. 2001, "Optical properties and
591 nondestructive estimation of anthocyanin content in plant leaves", *Photochemistry*
592 *and photobiology*, vol. 74, no. 1, pp. 38-45.
- 593 Goodenough, D.G., Dyk, A., Niemann, K.O., Pearlman, J.S., Chen, H., Han, T.,
594 Murdoch, M. & West, C. 2003, "Processing Hyperion and ALI for forest
595 classification", *IEEE Transactions on Geoscience and Remote Sensing*, vol. 41, no.
596 6 PART I, pp. 1321-1331.
- 597 Goodenough, D.G., Quinn, G.S., Gordon, P.L., Niemann, K.O. & Chen, H. 2011,
598 "Linear and nonlinear imaging spectrometer denoising algorithms assessed through
599 chemistry estimation", , pp. 4320.
- 600 Guyot, G., Baret, F. & Major, D.J. 1988, "High spectral resolution: Determination of
601 spectral shifts between the red and the near infrared", *International Archives of*
602 *Photogrammetry and Remote Sensing*, vol. 11, pp. 740-760.
- 603 Hardisky, M.A., Klemas, V. & Smart, R.M. 1983, "The influence of soil salinity,
604 growth form, and leaf moisture on the spectral radiance of *Spartina alterniflora*

- 605 canopies.", *Photogrammetric Engineering & Remote Sensing*, vol. 49, no. 1, pp.
606 77-83.
- 607 Hoel, B.O. 1998, "Use of a hand-held chlorophyll meter in winter wheat: Evaluation of
608 different measuring positions on the leaves", *Acta Agriculturae Scandinavica -
609 Section B Soil and Plant Science*, vol. 48, no. 4, pp. 222-228.
- 610 Horvitz, L. 1982, "Near-surface evidence of hydrocarbon movement from depth" in
611 *Problems of petroleum migration*, eds. W.H. Roberts & R.J. Cordell, AAPG
612 Studies in Geology 10 edn, American Association of Petroleum Geologists, Tulsa,
613 Oklahoma, USA, pp. 241-263.
- 614 Horvitz, L. 1985, "Geochemical exploration for petroleum", *Science*, vol. 229, no. 4716,
615 pp. 821-827.
- 616 Huete, A.R., Liu, H.Q., Batchily, K. & Van Leeuwen, W. 1997, "A comparison of
617 vegetation indices over a global set of TM images for EOS-MODIS", *Remote
618 Sensing of Environment*, vol. 59, no. 3, pp. 440-451.
- 619 Hunt Jr, E.R. & Rock, B.N. 1989, "Detection of changes in leaf water content using
620 Near- and Middle-Infrared reflectances", *Remote Sensing of Environment*, vol. 30,
621 no. 1, pp. 43-54.
- 622 Hurtig, A.K. & San-Sebastián, M. 2005, "Epidemiology vs epidemiology: The case of
623 oil exploitation in the Amazon basin of Ecuador [5]", *International journal of
624 epidemiology*, vol. 34, no. 5, pp. 1170-1172.
- 625 Jago, R.A., Cutler, M.E.J. & Curran, P.J. 1999, "Estimating canopy chlorophyll
626 concentration from field and airborne spectra", *Remote Sensing of Environment*,
627 vol. 68, no. 3, pp. 217-224.
- 628 Kaufman, Y.J. & Tanre, D. 1992, "Atmospherically resistant vegetation index (ARVI)
629 for EOS-MODIS", *IEEE Transactions on Geoscience and Remote Sensing*, vol. 30,
630 no. 2, pp. 261-270.
- 631 Kooistra, L., Leuven, R.S.E.W., Wehrens, R., Nienhuis, P.H. & Buydens, L.M.C. 2003,
632 "A comparison of methods to relate grass reflectance to soil metal contamination",
633 *International Journal of Remote Sensing*, vol. 24, no. 24, pp. 4995-5010.
- 634 Larcher, W. 2003, *Physiological Plant Ecology*, Fourth edn, Springer, Germany.
- 635 Lichtenthaler, H.K., Lang, M., Sowinska, M., Heisel, F. & Miehe, J.A. 1996, "Detection
636 of vegetation stress via a new high resolution fluorescence imaging system",
637 *Journal of Plant Physiology*, vol. 148, no. 5, pp. 599-612.
- 638 Malhi, Y., Roberts, J.T., Betts, R.A., Killeen, T.J., Li, W. & Nobre, C.A. 2008,
639 "Climate change, deforestation, and the fate of the Amazon", *Science*, vol. 319, no.
640 5860, pp. 169-172.

- 641 Marengo, R.A., Antezana-Vera, S.A. & Nascimento, H.C.S. 2009, "Relationship
642 between specific leaf area, leaf thickness, leaf water content and SPAD-502
643 readings in six Amazonian tree species", *Photosynthetica*, vol. 47, no. 2, pp. 184-
644 190.
- 645 Martin, P.L. 2011, "Global governance from the amazon: Leaving oil underground in
646 Yasuní National park, Ecuador", *Global Environmental Politics*, vol. 11, no. 4, pp.
647 22-42.
- 648 Marx, E. 2010, "The fight for Yasuni", *Science*, vol. 330, no. 6008, pp. 1170-1171.
- 649 Ministerio de Energia y Minas 2001, *Reglamento Ambiental para Operaciones*
650 *Hidrocarburíferas en el Ecuador*, Decreto Ejecutivo 1215 edn, Registro oficial
651 265, Ecuador.
- 652 Mutanga, O., Skidmore, A.K. & Prins, H.H.T. 2004, "Predicting in situ pasture quality
653 in the Kruger National Park, South Africa, using continuum-removed absorption
654 features", *Remote Sensing of Environment*, vol. 89, no. 3, pp. 393-408.
- 655 Noomen, M.F. 2007, *Hyperspectral Reflectance of vegetation affected by underground*
656 *hydrocarbon gas seepage*, PhD edn, International Institute for Geo-Information
657 Science & Earth Observation-ITC, Enschede-The Netherlands.
- 658 Noomen, M.F. & Skidmore, A.K. 2009, "The effects of high soil CO₂ concentrations on
659 leaf reflectance of maize plants", *International Journal of Remote Sensing*, vol. 30,
660 no. 2, pp. 481-497.
- 661 Noomen, M.F., Skidmore, A.K., van der Meer, F.D. & Prins, H.H.T. 2006, "Continuum
662 removed band depth analysis for detecting the effects of natural gas, methane and
663 ethane on maize reflectance", *Remote Sensing of Environment*, vol. 105, no. 3, pp.
664 262-270.
- 665 Noomen, M.F., Smith, K.L., Colls, J.J., Steven, M.D., Skidmore, A.K. & Van Der
666 Meer, F.D. 2008, "Hyperspectral indices for detecting changes in canopy
667 reflectance as a result of underground natural gas leakage", *International Journal*
668 *of Remote Sensing*, vol. 29, no. 20, pp. 5987-6008.
- 669 Noomen, M.F., van der Werff, H.M.A. & van der Meer, F.D. 2012, "Spectral and
670 spatial indicators of botanical changes caused by long-term hydrocarbon seepage",
671 *Ecological Informatics*, vol. 8, pp. 55-64.
- 672 Penuelas, J., Filella, I., Lloret, P., Munoz, F. & Vilajeliu, M. 1995, "Reflectance
673 assessment of mite effects on apple trees", *International Journal of Remote*
674 *Sensing*, vol. 16, no. 14, pp. 2727-2733.
- 675 Peñuelas, J., Piñol, J., Ogaya, R. & Filella, I. 1997, "Estimation of plant water
676 concentration by the reflectance Water Index WI (R900/R970)", *International*
677 *Journal of Remote Sensing*, vol. 18, no. 13, pp. 2869-2875.

- 678 Pimstein, A., Eitel, J.U.H., Long, D.S., Mufradi, I., Karnieli, A. & Bonfil, D.J. 2009, "A
679 spectral index to monitor the head-emergence of wheat in semi-arid conditions",
680 *Field Crops Research*, vol. 111, no. 3, pp. 218-225.
- 681 Rochlin, J. 2011, "Development, the environment and ecuador's oil patch: The context
682 and nuances of the case against Texaco", *Journal of Third World Studies*, vol. 28,
683 no. 2, pp. 11-39.
- 684 Rondeaux, G., Steven, M. & Baret, F. 1996, "Optimization of soil-adjusted vegetation
685 indices", *Remote Sensing of Environment*, vol. 55, no. 2, pp. 95-107.
- 686 Rosso, P.H., Pushnik, J.C., Lay, M. & Ustin, S.L. 2005, "Reflectance properties and
687 physiological responses of *Salicornia virginica* to heavy metal and petroleum
688 contamination", *Environmental Pollution*, vol. 137, no. 2, pp. 241-252.
- 689 Rouse, J.W., Haas, R.H. & Schell, J.A. 1974, "Monitoring the Vernal Advancement of
690 Retrogradation of Natural Vegetation", .
- 691 Sánchez-Azofeifa, G.A., Castro, K., Wright, S.J., Gamon, J., Kalacska, M., Rivard, B.,
692 Schnitzer, S.A. & Feng, J.L. 2009, "Differences in leaf traits, leaf internal structure,
693 and spectral reflectance between two communities of lianas and trees: Implications
694 for remote sensing in tropical environments", *Remote Sensing of Environment*, vol.
695 113, no. 10, pp. 2076-2088.
- 696 Shumacher, D. 1996, "*Hydrocarbon-induced alteration of soils and sediments*" in
697 *Hydrocarbon migration and its near-surface expression: APPG Memoir 66*, eds. D.
698 Shumacher & M.A. Abrams, pp. 71-89.
- 699 Sims, D.A. & Gamon, J.A. 2002, *Relationships between leaf pigment content and*
700 *spectral reflectance across a wide range of species, leaf structures and*
701 *developmental stages*.
- 702 Smith, K.L., Steven, M.D. & Colls, J.J. 2004, "Remote sensing techniques for
703 monitoring plant stress responses to gas leaks", *International Gas Research*
704 *Conference Proceedings*, .
- 705 Smith, K.L., Colls, J.J. & Steven, M.D. 2005, *A Facility to Investigate Effects of*
706 *Elevated Soil Gas Concentration on Vegetation*, Springer Netherlands.
- 707 Smith, K.L., Steven, M.D. & Colls, J.J. 2005, "Plant spectral responses to gas leaks and
708 other stresses", *International Journal of Remote Sensing*, vol. 26, no. 18, pp. 4067.
- 709 Smith, K.L., Steven, M.D. & Colls, J.J. 2004, "Use of hyperspectral derivative ratios in
710 the red-edge region to identify plant stress responses to gas leaks", *Remote Sensing*
711 *of Environment*, vol. 92, no. 2, pp. 207-217.
- 712 Steven, M.D., Malthus, T.J., Demetriades-Shah, T.H., Danson, F.M. & Clark, J.A.
713 1990, "High-spectral resolution indices for crop stress", *Applications of remote*
714 *sensing in agriculture*, , pp. 209-227.

- 715 Tedersoo, L., Sadam, A., Zambrano, M., Valencia, R. & Bahram, M. 2010, "Low
716 diversity and high host preference of ectomycorrhizal fungi in Western Amazonia,
717 a neotropical biodiversity hotspot", *ISME Journal*, vol. 4, no. 4, pp. 465-471.
- 718 Vallejo, M.C., Burbano, R., Falconí, F. & Larrea, C. 2015, "Leaving oil underground in
719 Ecuador: The Yasuní-ITT initiative from a multi-criteria perspective", *Ecological*
720 *Economics*, vol. 109, no. 0, pp. 175-185.
- 721 van der Meer, F., Yang, H. & Kroonenberg, S. 2006, "Imaging spectrometry and
722 petroleum geology" in *Imaging Spectrometry*, eds. F. van der Meer & S.M. de
723 Jong, Springer, Dordrecht, The Netherlands, pp. 219-241.
- 724 Vile, D., Garnier, É., Shipley, B., Laurent, G., Navas, M.-., Roumet, C., Lavorel, S.,
725 Díaz, S., Hodgson, J.G., Lloret, F., Midgley, G.F., Poorter, H., Rutherford, M.C.,
726 Wilson, P.J. & Wright, I.J. 2005, "Specific leaf area and dry matter content
727 estimate thickness in laminar leaves", *Annals of Botany*, vol. 96, no. 6, pp. 1129-
728 1136.
- 729 Vogelmann, J.E., Rock, B.N. & Moss, D.M. 1993, "Red edge spectral measurements
730 from sugar maple leaves", *International Journal of Remote Sensing*, vol. 14, no. 8,
731 pp. 1563-1575.
- 732 White, J.W. & Montes-R, C. 2005, "Variation in parameters related to leaf thickness in
733 common bean (*Phaseolus vulgaris* L.)", *Field Crops Research*, vol. 91, no. 1, pp. 7-
734 21.
- 735 Yang, H. 1999, *Imaging Spectrometry for Hydrocarbon Microseepage*, Delf
736 University of Technology.
- 737 Yang, H., Zhang, J., Van Der Meer, F. & Kroonenberg, S.B. 2000, "Imaging
738 spectrometry data correlated to hydrocarbon microseepage", *International Journal*
739 *of Remote Sensing*, vol. 21, no. 1, pp. 197-202.
- 740 Zarco-Tejada, P.J., Miller, J.R., Mohammed, G.H. & Noland, T.L. 2000, "Chlorophyll
741 fluorescence effects on vegetation apparent reflectance: I. Leaf-level measurements
742 and model simulation", *Remote Sensing of Environment*, vol. 74, no. 3, pp. 582-
743 595.
- 744 Zhu, L., Zhao, X., Lai, L., Wang, J., Jiang, L., Ding, J., Liu, N., Yu, Y., Li, J., Xiao, N.,
745 Zheng, Y. & Rimmington, G.M. 2013, "Soil TPH Concentration Estimation Using
746 Vegetation Indices in an Oil Polluted Area of Eastern China", *PLoS ONE*, vol. 8,
747 no. 1.
- 748 Zweifel, R., Rigling, A. & Dobbertin, M. 2009, *Species-specific stomatal response of*
749 *trees to drought - A link to vegetation dynamics?*.
- 750